공학석사학위논문

Numerical study on neoclassical tearing mode stabilization via minimum growth rate seeking method

최소 증가율 탐색 기법을 이용한 신고전 찢어짐 모드 안정화에 대한 전산모사적 연구

2014년 2월

서울대학교 대학원

에너지시스템공학부

김 민 화

Numerical study on neoclassical tearing mode stabilization via minimum growth rate seeking method

최소 증가율 탐색 기법을 이용한
신고전 찢어짐 모드 안정화에 대한 전산모사적 연구

지도 교수 나 용 수

이 논문을 공학석사 학위논문으로 제출함
2014년 2월

서울대학교 대학원
에너지시스템공학부
김 민 화

김민화의 공학석사 학위논문을 인준함
2014년 2월

위 원 장 함 택 수 (인)

부위원장 나 용 수 (인)

위 원 황 용 석 (인)

Abstract

Numerical study on neoclassical tearing mode stabilization via minimum growth rate seeking method

Kim, Minhwa
Department of Energy Systems Engineering
Seoul National University

Neoclassical tearing mode (NTM) is one of critical instabilities which need to be stabilized to achieve high fusion performance. It degrades plasma confinement and sometimes can cause plasma disruptions. Injecting a localized electron cyclotron current drive (ECCD) has been proven experimentally as an effective method to stabilize NTM by replacing the missing bootstrap current in the island. As the efficiency of this method strongly depends on the alignment between the island and the beam deposition, real-time feedback control is essential to achieve robust suppression of NTM.

In this thesis, a concept of minimum growth rate seeking control is proposed and the feedback control of the growth rate of the magnetic island is shown to

be faster and more efficient than that of the island width. As the minimum growth rate seeking method is a non-model-based control method, it has advantages of no requirement of precise real-time equilibrium reconstruction and EC ray-tracing calculation or NTM plasma system identification.

An integrated numerical model is setup for time-dependent simulations of NTM evolution where plasma equilibrium, transport, and heating and CD by EC are coupled with the solver of simplified Rutherford equation in a self-consistent way. It is applied to KSTAR plasmas for reproducing the evolution of the island width in a NTM stabilization experiment.

To evaluate the performance of the growth rate control concept, predictive feedback control simulations are performed based on two types of minimum seeking controller in KSTAR; finite difference method (FDM) and sinusoidal perturbation. Realistic control input and output parameters are used as the format of measured island growth rates from diagnostics and the poloidal launcher angle, respectively. The results are compared with the minimum island width seeking method. It is revealed that the proposed control concept is less limited in minimum seeking and more robust in reducing misalignment in shorter time scales.

Keywords: Neoclassical tearing mode, Magnetic island, NTM stabilization, Minimum seeking control, Electron cyclotron current drive (ECCD)

Student Number: 2012-20988

Contents

List of Tables

List of Figures

Chapter 1

Introduction

1.1 Neoclassical tearing mode (NTM)

Neoclassical tearing mode (NTM) is well known resistive MHD instability which is driven by the helical perturbation of bootstrap current density making the isolated magnetic island in the flux surface. Resistivity of plasma makes it possible the occurrence of the magnetic reconnection which has its source in the free energy from the current density perturbation. The island-like magnetic flux is made as a result. When this magnetic island size is sufficiently large, it can be the 'seed' island. This seed island causes the secondary loss of the bootstrap current density which is driven by neoclassical effect. The magnetic island from NTM grows with this perturbation of bootstrap current density. [1]

The magnetic islands from NTM limit the achievable plasma beta value and can cause the plasma disruption. The magnetic surface usually separated and does not meet each other. Since the particles move along the magnetic field line, separated magnetic flux make it difficult for the particle or energy to transport radially which is perpendicular with the magnetic surface. The magnetic island is formed by the magnetic reconnection between distinguished magnetic flux surfaces. Therefore, this enhances the particle and energy radial transport by making the shortcut between the magnetic surfaces.

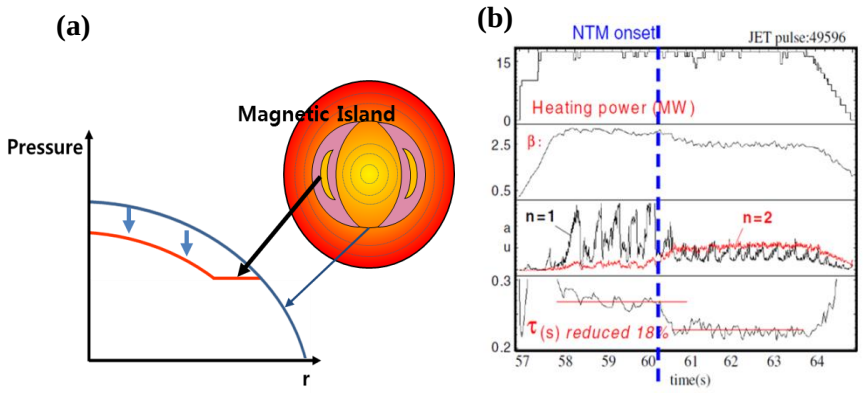

Figure 1.1 The adverse effect of NTM on (a) flattening of pressure profile and (b) degrading the energy confinement time (τ_E) observed in JET [2].

The figure 1.1 shows the magnetic islands within the magnetic flux surface and their effects on the confinement. The plasma radial profiles such as the temperature or pressure are flattened by this high radial transport. It degrades the plasma confinement performance and limits the beta to be increased as a result. Because of this, the stabilization of the NTM is issue for tokamaks such as KSTAR and even ITER. [1]

1.2 Stabilization of NTM

Injecting ECCD into the magnetic island is most popular method for stabilization of NTM. There are many ways to stabilize the NTM. One is to remove the trigger of seed islands. Usually this seed island is generated by other MHD activities such as the sawtooth. The other is to remove the destabilizing energy source of NTM. Since the NTM is usually destabilized

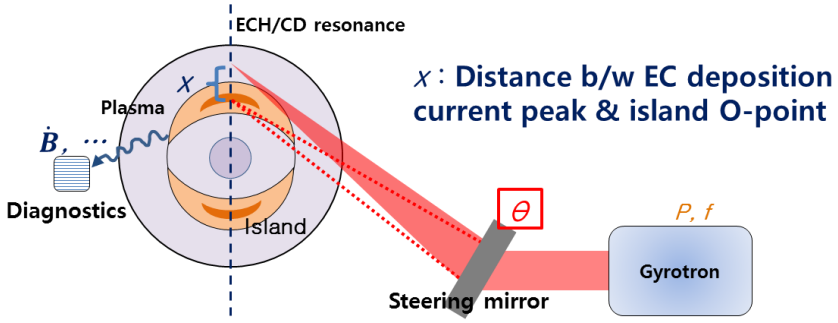

Figure 1.2 Method of NTM stabilization using ECCD and major parameters (x : Misalignment between beam and island O-point, θ : EC beam poloidal angle, P : Power of EC beam, f : Modulation frequency of EC beam).

by the loss of the bootstrap current density, replacing this current loss with other externally driven current can stabilize the NTM. Various current drive sources are possible. The most promising method is to use the Electron Cyclotron Current Drive (ECCD) which utilizes the resonance between electron's cyclotron motion and the waves due to its good beam localization. This stabilization method is successfully proven on D3-D [3,4] and JT-60U[5,6] etc. for m/n=3/2 NTMs. By injecting ECCD into the magnetic island O-point which is center of magnetic island, it can be stabilized.

For efficient stabilization of NTM many parameters exist to run ECCD and the misalignment between this ECCD deposition position and magnetic island O-point is one of them. The poloidal launcher angle of injected EC beam determines this misalignment moving along the resonance zone like figure 1.2. Since NTM stabilization using ECCD requires, at least, driving current around island O-point, knowing the proper poloidal launcher angle is

essential to inject ECCD on right position. Furthermore, the efficiency of stabilization is also affected by the misalignment so that even ECCD can destabilize the magnetic island when it is large enough.[7] Therefore, align EC well to magnetic island and track the time variation of island position is very necessary to stabilize NTM robustly.

Various strategies exist to obtain proper poloidal launcher angle. The control using the plasma real-time reconstruction is well known one of these control methods. This requires many measurements for the NTM position detection in ρ, plasma equilibrium reconstruction and EC ray-tracing calculation. This aligns the estimated rational surface position where the magnetic islands exist and the calculated ECCD peak position using these information. The poloidal launcher angle is adjusted by monitoring this alignment level with real-time feedback. This can be robust in various plasma conditions when the soundness of measurements and the calculations can be ensured. However, this requires difficult and massive measurements and calculations such as equilibrium reconstruction and real-time ray-tracing calculation which takes at least 40ms although it is reduced.[8] As a result, the control time increases and the misalignment from the estimation error can be happened.[9]

The other strategies are heuristic methods which monitor the magnetic island width variation with respect to the variation of beam position or poloidal launcher angle. The ‘Search and Suppress’ is most successful control method in experiments.[9] Control strategy using the minimum seeking technique is also proposed recent years.[10,11] The minimum seeking control

is the method to find the minimum point of the input so that deduce proper output which make input to be minimized. Assuming that the magnetic island width is function of misalignment, the width is minimized using sinusoidal perturbation based minimum seeking control. This method shows better performance than the ‘Search and Suppress’ method from the simulations in previous research. Because it requires only the width of magnetic island (even with the noise) as the control input, this method can be useful to overcome the errors of method using real-time plasma reconstruction and to develop the NTM stabilization method for tokamaks which need fast control or undergo difficulties to realize the good real-time reconstruction system because of the lack of experience, cost or tough environment to measure precisely such as ITER.

1.3 Motivations

Although the strategy of NTM stabilization using the minimum width seeking control was successful which minimizes magnetic island width via minimum seeking technique, the minimum relation between width and EC misalignment becomes somewhat unclear when the control loop time is small enough than the island width saturation time. The island width is minimized by changing the misalignment to reduce the width. When the growth rate is negative, the island width is always decreasing regardless of the value of

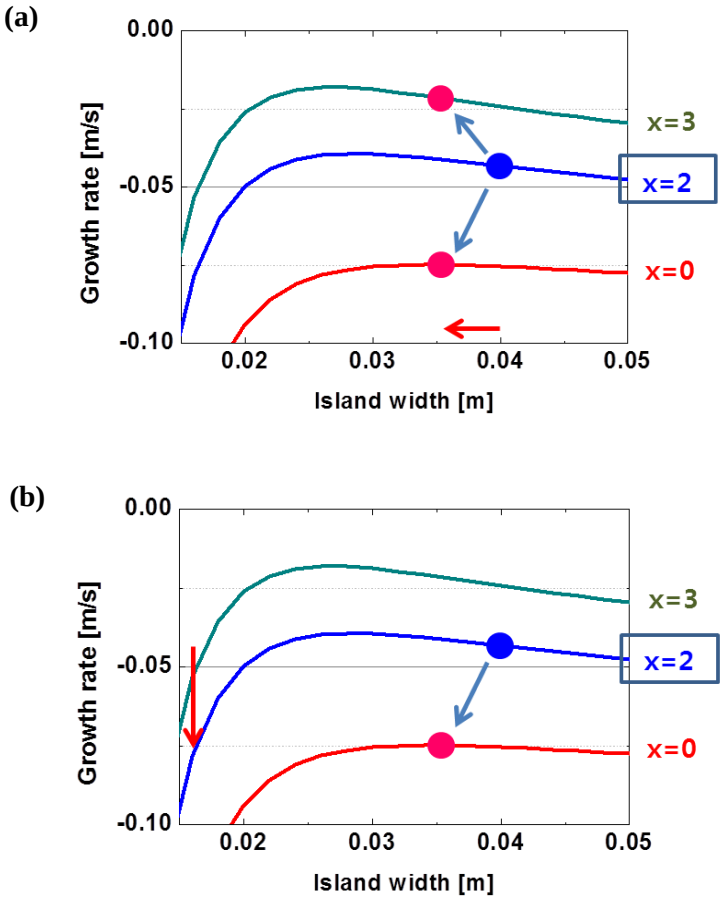

Figure 1.3 Example of heuristic misalignment control starting from the blue point to the red point (a) using the minimum width seeking method which the next step can have various solution and (b) using minimum growth rate seeking method which the next step has unique solution.

misalignment like figure 1.3(a). This means that the minimizing procedure cannot have unique solution although the decreasing misalignment is most favorable and the minimum relation between them is hard to catch. In previous research, they extract the minimum relation with sinusoidal perturbation based controller.

However, when the growth rate is considered as the input parameter of controller, the problem can be easier to solve. Generally, the growth rate is known as to decrease as the misalignment decreases due to the increase of EC stabilizing effect. Assuming that EC power is large enough to affect magnetic island width evolution than other plasma parameters and control time interval is small enough to ignore the time variation of growth rate minimum value, the island width growth rate is decreased as the misalignment is reduced and has clear minimum relationship with misalignment. The controller can find right direction to move the misalignment because of that like figure 1.3(b). Also, minimizing growth rate means fastest magnetic suppression. Therefore, minimum growth rate seeking control concept can be more easy, accurate and efficient strategy to stabilization of NTM than minimum width seeking control concept.

In addition, the NTM stabilization simulations using this minimum width seeking controller have been performed with relatively unrealistic conditions. The island width value and misalignment is used as the input and output parameter for controller with fixed plasma conditions such as EC driven current density peak value and so on. However, the NTM width is usually just estimated using the mirnov coil which detects the time variation of magnetic

field in rotating plasma not measured directly in experiment. The false measurement of island width can occur as a result unless the plasma conditions are fixed. As the output result, the poloidal beam angle is needed not the misalignment. Due to effects of the change of EC deposition with poloidal angle and the time-dependent variation plasma, stabilization simulation with estimated information of island width and poloidal angle for input, output parameter can reflect more realistic condition unlike previous studies.

1.4 Objectives and scope of this work

Two of the improvement issues are mentioned in the previous section. The objective of this work is to investigate the effectiveness of the minimum growth rate seeking control concept for NTM stabilization using measured island growth rate and poloidal launcher angle as the input and output respectively in time-dependent plasma environment for more realistic simulation. There are two works for this objective. One is to establish reasonable time-dependent numerical system. Investigation of effectiveness of the proposed control concept is the other.

In chapter 2, the theoretical backgrounds of the NTM stabilization using the minimum seeking method is reviewed briefly for understanding. First, the methodology of minimum seeking control is introduced. The effects of EC on NTM evolution is followed briefly. It can be known the possibility of NTM

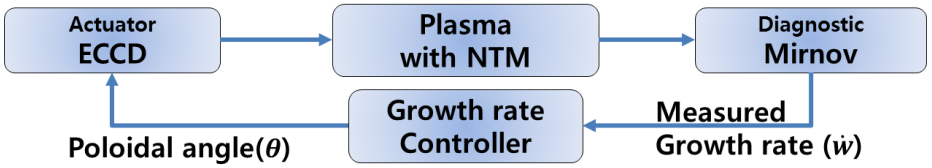

Figure 1.4 Conceptual diagram of NTM stabilization numerical system compose with NTM plasma as the plant, mirnov coil measurement as diagnostic, ECCD as the actuator and minimum growth rate seeking controller as the feedback control

stabilization using minimum seeking method based on these NTM theories.

In Chapter 3, the numerical system for NTM control simulations with integrated modeling is tested with experiment results in KSTAR. The NTM stabilization experiments are analyzed and the magnetic island width evolution in experiment simulated. By comparing the experiment result and simulation result, the soundness of numerical system can be tested.

In chapter 4, the NTM stabilization simulation using minimum growth rate seeking control method is performed with realistic control parameter in time-dependent plasma conditions. To confirm the effectiveness of this proposed control concept, two type of controller; finite difference method (FDM) based minimum seeking controller and sinusoidal perturbation based minimum seeking controller are introduced. The results are compared with that of simulation using minimum width seeking control method in same way.

The final chapter summarizes all the results, and then a conclusion of this work is presented. The expectation is followed.

Chapter 2

Background of NTM stabilization via minimum seeking method

2.1 Principle of minimum seeking method

In general control problems, there exists the control target to achieve for the system. However, in the control problems which require that the system regulates around its minimum performance state, the precise target value cannot be exist. These problems need different method with conventional solutions such as physical model based PID(proportional-integral-differential) control due to this unknowableness of target.

The minimum seeking control can achieve their control goal with non-model based adaptive method. The feedback control is performed by measuring the input and output value. The system's performance parameter becomes the input and the system's state which determines the performance becomes output of controller. We can find the minimum value of input by keeping moving the output to decreasing direction of input.[12] Assume that the system has the minimum. The decreasing direction can be obtained from the gradient between the input and output since it has different sign of gradient around the minimum point like the figure 2.1. Therefore the moving direction of output is determined by the gradient between the input and output

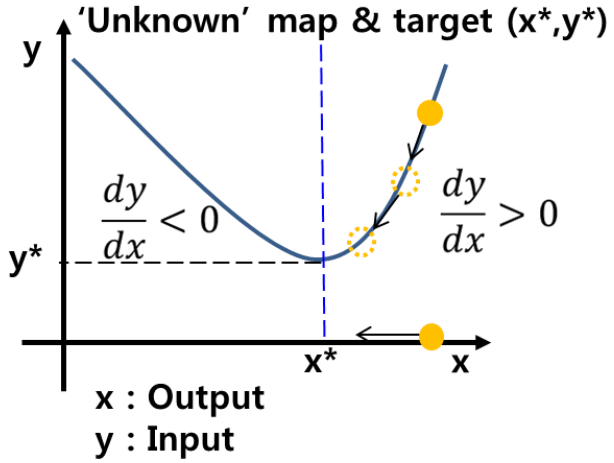

Figure 2.1 An illustration of minimum seeking dynamics

and also the magnitude of moving step is usually determined proportional to this gradient which is the steepest decent method.[13]

$$\dot{x} = K(\frac{dy}{dx}) \tag{2.1}$$

Here the x is output parameter, y is input parameter and K is adaptive gain.

This gradient can be obtained in various ways. The simplest and powerful way to determine the gradient is the method using finite difference method (FDM). Basically, the gradient can be evaluated from the input value variation with respect to the output value variation. The change of output in next time step makes that of the input. The gradient can be detected directly by measuring them.

$$\frac{dy}{dt}/\frac{dx}{dt} = \frac{dy}{dx} = \frac{y_{i+1}-y_i}{x_{i+1}-x_i} \tag{2.2}$$

Using the steepest decent method as the adaptive control law, the error of

output to the unknown target value can decrease as a result for negative adaptive gain, K. [13]

$$\dot{e} = \dot{y} - \dot{y}* = \dot{y} = \frac{dy}{dx}\dot{x} = K\left(\frac{dy}{dx}\right)^2 < 0 \;\; for \;\; K < 0 \tag{2.3}$$

Here $\mathrm{y}*$ is unknown target of y and e is the error of them.

The other way is the perturbation based minimum seeking method. This method introduces probing dithering signal to the output. The sinusoidal perturbation is usually used as this probing signal. The system performance responses with this dithering system's state so that the dithering input is generated by output perturbation.

$$x(t) = x* - e(t) \tag{2.4}$$

$$X(t) = x(t) + a\,sin(wt) \tag{2.5}$$

$$y(t) = f\big(x(t)\big) = y* + \frac{f''}{2}(a\,sin(wt) - e(t))^2$$

$$= \mathrm{y}* + \frac{\mathrm{f}''}{2}((\mathrm{a}\sin(\mathrm{wt}))^2 - 2\mathrm{ae(t)}\sin(\mathrm{wt}) + \mathrm{e(t)}^2)$$

$$= \mathrm{y}* + \frac{\mathrm{f}''}{2}\left(\frac{\mathrm{a}^2}{2}(1 - \cos(2\mathrm{wt})) - 2\mathrm{ae(t)}\sin(\mathrm{wt}) + \mathrm{e(t)}^2\right) \tag{2.6}$$

Here, e is error of output x to the unknown target of $x*$, X is output signal which the sinusoidal perturbation is added, the f is mapping of x and y, a is the positive amplitude of sinusoidal signal and w is the perturbation frequency before adding sinusoidal perturbation. The resulting input signal, y is high pass filtered and multiplied with same sinusoidal perturbation to obtain the magnitude of sinusoidal perturbation term of that.

$$y1(t) = \frac{f''}{2}\left(-\frac{a^2}{2}\cos(2wt)\sin(wt) - 2ae(t)(\sin(wt))^2 + e(t)^2\sin(wt)\right)$$

$$= \frac{f''}{2}\left(-\frac{a^2}{2}\cos(2wt)\sin(wt) - ae(t)(1-\cos(2wt)) + e(t)^2\sin(wt)\right) \quad (2.7)$$

Here y1 is the resulting signal. After low pass filtering or integrating of that to attenuate other harmonic signals, the output g is as follow.

$$g = -ae(t)\frac{f''}{2} \quad (2.8)$$

Here the controller is already assumed to be around its target so that the first order derivative is zero. The resulting g is proportional to the error and second derivative.

$$\dot{x} = Kg = -aKe(t)\frac{f''}{2}$$

$$= \dot{x} * -\dot{e} = -\dot{e} = -aKe(t)\frac{f''}{2} \quad (2.9)$$

The output *x* is estimated with steepest decent method. This also makes the output error to the unknown target to decrease.

$$\dot{e} = aKe(t)\frac{f''}{2} < 0 \;\; for \;\; K < 0 \quad (2.10)$$

When the error is negative, the time derivative of that need to increase to converge to zero and the same condition of adaptive gain K is obtained.

This method can detect the gradient efficiently in environment with disturbance. And it is easy to add the control parameters since the perturbation frequency help to distinguish each other. [14]

2.2 NTM stabilization via minimum seeking method

The evolution of magnetic island width is usually described with the Rutherford equation.[1,15]

$$\frac{\tau_R}{r_s}\frac{dW}{dt} = \sum r_s\Delta_i' = r_s\Delta_0' + r_s\Delta_{EC}' + \cdots \quad (2.11)$$

Here W is full width of magnetic island, $\tau_R$is the local resistive time from Spitzer resistivity, r_s is the minor radius of mode rational surface, Δ' is the stability index which is related to the perturbation of current density source. The terms related with EC generally stabilize the NTM. Their magnitude is affected by the misalignment between the EC deposition position and magnetic island O-point which is usually the center of that. First, the EC can correct the classical stability index, Δ_0' which is induced from the equilibrium current profile. The small, well localized current density perturbation from the EC change the profile around the rational surface to stabilize the mode

$$r_s\delta\Delta_0' \propto -\frac{j_{EC}}{\delta_{EC}}F(x,\delta_{EC}) \quad (2.12)$$

Here $r_s\delta\Delta_0'$ is the correction term, j_{EC} is current density peak value for Gaussian profile, δ_{EC} is the full width half-maximum (FWHM) of EC driven current profile and F is the function of δ_{EC} and the misalignment $x = r_{EC} - r_s$ which is related with plasma dispersion function. This function F is generally increased as the misalignment is reduced like the figure 2.2. [16] The other effect of EC is to replace the missing bootstrap current.

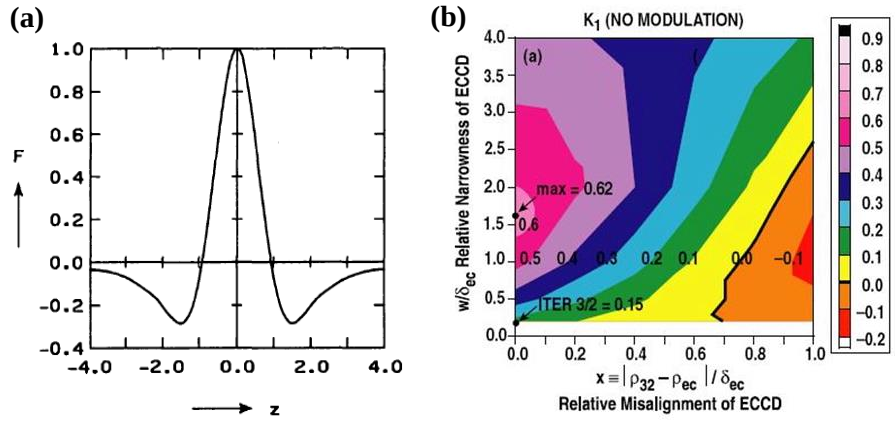

Figure 2.2 Efficiency function of ECCD on Rutherford equation : (a) Profile function F($z = {}^{x}/_{\delta_{EC}}$) [16] , (b) Contour of $K1$[17]

$$r_s \Delta'_{ECCD} \propto -\frac{j_{EC}}{W} K1(W, x, \delta_{EC}) \tag{2.12}$$

Here $K1$ which determines the efficiency of ECCD is the function of island width, misalignment, driven current profile FWHM. The efficiency of this effect varies with island width but also generally increases as the misalignment decreases. [17] Consequently, the mode is more stabilized as this misalignment decreases and the overall mode growth rate is reduced.

This misalignment is changed by the injected EC beam poloidal angle. This means that the growth rate can be varied by changing the poloidal angle although the relation between misalignment and poloidal angle is nonlinear due to the dispersion relation of plasma. Therefore, the mode growth rate can have the minimum with respect to the poloidal angle value which make the misalignment to be zero. This makes it possible to introduce the minimum seeking control method to stabilize the NTM. By tuning the poloidal angle to minimize the growth rate, the misalignment can be reduced. However, the

minimum value of growth rate is slightly changed with variation of the island width in the NTM theory, the assumption is necessary that the growth rate variation from the misalignment is larger than that from the island width. Or following conditions have to be satisfied. [14]

$$FDM: K < \left(\frac{d\dot{W}}{dW}\right) \Big/ \left(\frac{d\dot{W}}{d\theta}\right)^2 \tag{2.13}$$

$$Sin.perturbation\ based\ method: sufficiently\ large\ w$$

Here, $\dot{W}$ is the island growth rate, θ is the poloidal angle. For sufficiently large w, there exists a unique exponentially stable periodic solution for time-variant minimum seeking.

Chapter 3

Integrated modeling of NTM evolution

3.1 Integrated numerical system for NTM simulations

To perform the control simulation, the virtual physical system is necessary which reflect the experimental situation well. For this heuristic control monitoring the island width information, the measurement of island width from the mirnov coil signal and EC beam poloidal angle are usually required as the input and output parameter in experiment. The magnetic islands from the NTM are rotating with plasma rotation. They generate the magnetic perturbation and they can be detected by mirnov coils based on faraday's law. After integrating and filtering out this signal with the mode frequency so that the background signals are removed, the amplitude of mode can be estimated. However, because the magnetic perturbation amplitude is affected by the plasma and mode conditions, this estimation is not the exact island width amplitude and it is expected as the simple theoretical calculation.[18]

$$\mathrm{W} = \left(\frac{4nr_s R_0}{msB_{\varphi 0}}\left(\frac{b}{r_s}\right)^{m+1} |B_\theta|_{wall}\right)^{1/2} \tag{3.1}$$

Here m is the poloidal mode number, n is the toroidal mode number, R_0 is the major radius, $B_{\varphi 0}$ is the toroidal magnetic field on magnetic axis, b is the minor radius to the mirnov coil position, $|B_\theta|_{wall}$ is the magnetic

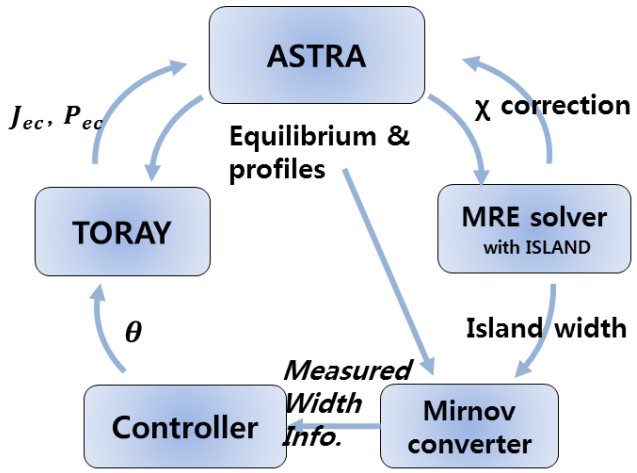

Figure 3.1 Integrated numerical system with the integrated modeling (ASTRA : plasma transport modeling, MRE solver : NTM width evolution modeling, TORAY : ECCD absorption and current drive modeling)

perturbation amplitude measured by mirnov coil at the wall and is the $s = r(dq/dr)/q$ magnetic shear.. As a result, measured island width information is disturbed by plasma variation. The EC absorption is also affected by plasma equilibrium etc. Therefore, the integrated numerial system should reflect the NTM plasma with variation and realize change of EC absorption by poloidal angle and plasma condition to simulate with realistic control condition.

The island width evolution is usually described by modified Rutherford equation (MRE) and this is focused on the neoclassical effect, polarization current effect and the ECH/CD effect in this work. [17,19]

$$\frac{\tau_R}{r_s}\frac{dW}{dt} = r_s\Delta_0' + r_s\delta\Delta_0'$$

$$+a_2 \frac{j_{bs}}{j_p}\frac{L_q}{W}\left[1-\frac{W_{marg}^2}{3W^2}-K_1\frac{j_{EC}}{j_{bs}}-\alpha_H F_H \frac{W}{W_{dep}}\frac{P_{EC}\eta_{EC}}{I_{EC}}\right] \quad (3.2)$$

Here W is full width of magnetic island, r_s is the minor radius of mode rational surface, $q = m/n$. τ_R is the local resistive time from Spitzer resistivity.

$$\tau_R = \mu_0 \sigma \kappa {r_s}^2 {T_e}^{3/2}/Z \quad (3.3)$$

Here σ is the Spitzer factor and κ is the elongation of the mode rational surface. Z is the effective charge number..

$r_s\Delta_0'$ is the classical tearing mode stability term and is assumed as a value of $-\mathrm{m}$ between marginal stability, 0 and strong stability, $-2\mathrm{m}$ which is mostly used for realistic mode evolution simulation. $r_s\delta\Delta_0'$ is the correction of classical stability index from the localized perturbation of equilibrium current profile by ECCD and considered as stabilizing effect. This is assumed as the Westerhof's model with no-island assumption and no modulation of EC beam.[16]

$$r_s\delta\Delta_0' \approx -\frac{5\pi^{3/2}}{32} a_2 \frac{L_q}{\delta_{EC}}\frac{j_{EC}}{j_p}F(e) \quad (3.4)$$

Here a_2 is the plasma geometrical factor which is calculated by ISLAND module.[20] $L_q = q/(dq/dr)$ is the magnetic shear scale length. j_{EC} is current density peak value and δ_{EC} is the full width half-maximum (FWHM) of EC driven current profile. j_p is the equilibrium parallel current density and $F(e)$ is evaluated as

$$F(e) = 1 - 2.43e + 1.40e^2 - 0.23e^3 \ \ for\ 0 \le e \le 2.25 \quad (3.5)$$

$$where\ \ e = \frac{|r_{EC} - r_s|}{\delta_{EC}}$$

The third term of right-hand side in Equation (3.2) means the destabilizing bootstrap current effect on island growth rate. j_{bs} is the unperturbed local bootstrap current density without an island. The forth term of right-hand side in Equation (3.2) means the stabilization effect of small island and the polarization threshold W_{marg}. is the marginal island size incorporates the this stabilization effect and assumed as twice of the ion banana width.[17]

$$W_{marg} \approx 2\epsilon^{1/2}\rho_{\theta i} \tag{3.6}$$

Here ϵ is the local inverse aspect ratio and $\rho_{\theta i} = \sqrt{2m_i k_B T_i / e^2 B_\theta^2}$ is the local poloidal ion gyro-radius. The fifth term of right-hand side in Equation (3.2) is the stabilizing ECCD effect by replacing missing bootstrap current and the effectiveness coefficient K_1 is determined by a matrix calculated from improved Perkin-Harvey's current drive model.[21] The last term of right-hand side in Equation (3.2) is the contribution of the EC heating[22] which is small when the ECCD is injected but necessary for more proper simulation.

The integrated numerical system is composed as the figure 3.1. The plasma variations in time are calculated by the 1.5D transport code ASTRA with equilibrium solver ESC. The EC absorption and driving current are calculated by the ray-tracing code, TORAY. The island width is calculated in MRE solver considering plasma profile variation with above model. They exchange the necessary information each other so that the self-consistent simulation is possible. The validity of this integrated numerical modeling can be tested by reproducing the experimental NTM plasma with ECCD which is

followed next. For control simulation, the mirnov converter and feedback controller are added. The mirnov converter changes island width from the MRE solver to the mirnov coil signal amplitude from the mode to consider the time-dependent plasma profile variation for the island width measurement. And the growth rate is calculated from the converted width information. The feedback controller deduces the poloidal angle using this growth rate from the converted island width information.

3.2 NTM stabilization experiment in KSTAR

Tearing modes appear frequently as the performance of KSTAR is enhanced and their stabilization using EC was tried in 2011 campaign. The pulse 6272 is the experiment in figure 3.2 which is injected EC with pre-estimation of mode appearance. The MHD mode is detected around t = 5.6 s. At the onset of mode, various events occur. The n=1 RMPs with 1.8 kA/turn were applied to affect ELM dynamics and their current was ramping down. The 110 GHz X2 mode EC and 170 GHz X3 mode EC were injected at t = 5.4 with the starting of RMP current ramp down. The power of EC was around 280 kW and 650 kW respectively. The plasma moved to the inward wall and collided around the EC injection suddenly. The loss of plasma sored energy and plasma current from the 0.6 MA to 0.4 MA was happened as a result of this event.

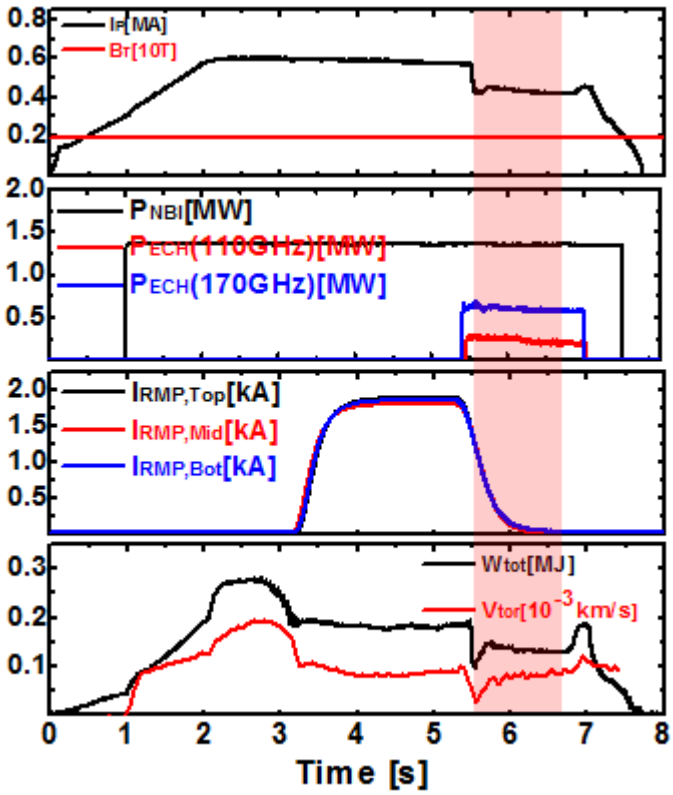

Figure 3.2 The overview of pulse 6272 in KSTAR experiment

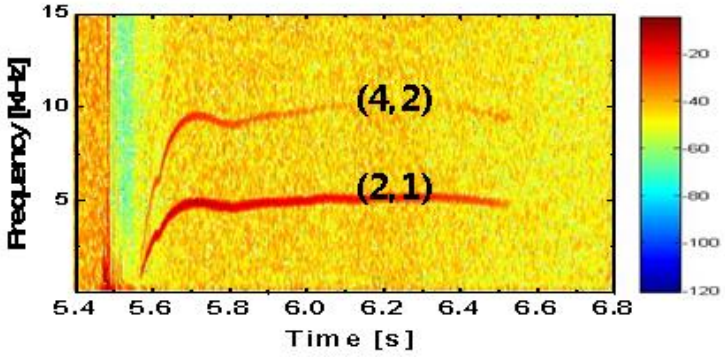

Figure 3.3 The spectrogram of mirnov coil(MCP03) for t = 6.4 s – 6.8 s

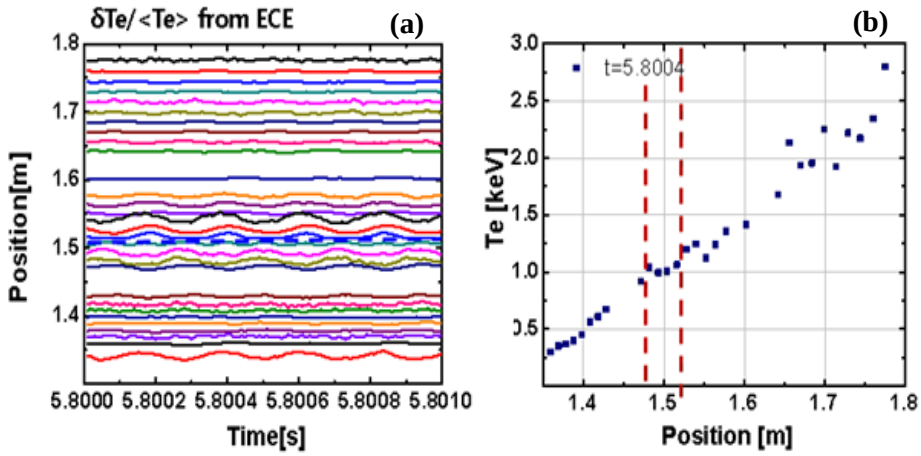

Figure 3.4 (a) Normalized electron perturbation data in time and location from ECE and blue dash line is expected island position. (b) Electron temperature profile from ECE and red dash line means the expected range of magnetic island

The m/n = 2/1 mode is detected after this event from the mirnov coils and this MHD mode can be known as tearing mode from the electron cyclotron emission (ECE) signals. Since the magnetic islands usually rotating with the plasma, the electron temperature perturbations have 180 degree phase inversion around the island O-point position due to the flattening effect of magnetic island. The mode was located around R = 1.5 m in major radius and the flattening in electron temperature profile was observed as a result.

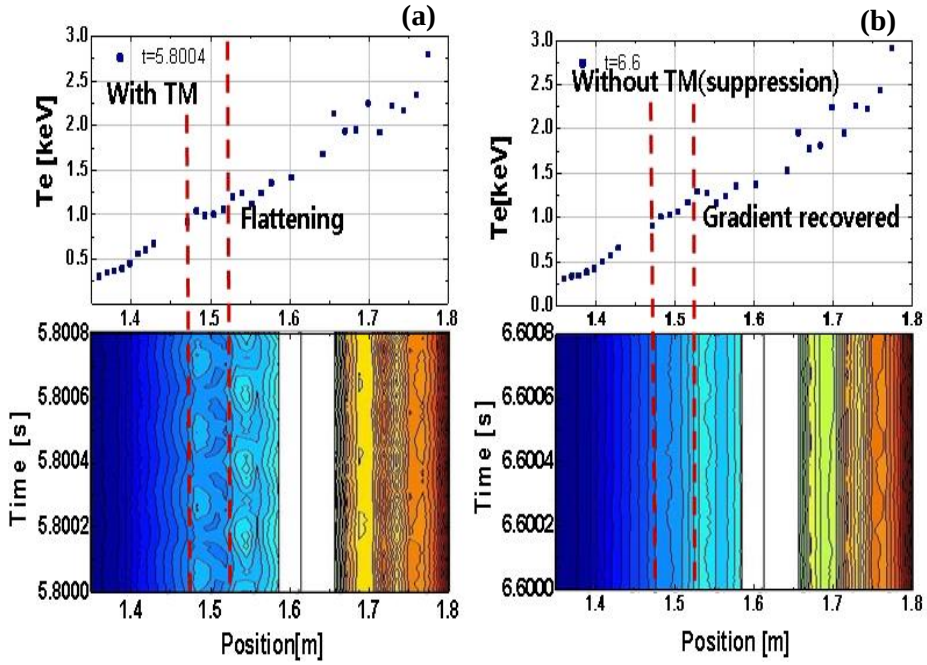

Figure 3.5 Electron temperature profile and its contour in time and position (a) before the mode disappearance and (b) after the mode disappearance.

The 110 GHz EC was aligned around the mode position. The amplitude of mode decreased gradually and the mode was finally disappeared around t = 6.55 s. The recovery of the gradient of electron temperature profile was observed after mode disappearance consequently. This is expected as the effect of EC injection comparing with other experiment with tearing mode but without EC injection.

3.3 Validation of the integrated numerical system with experiment

The validity of the integrated numerical system can be tested by reproducing the experimental island width evolution with EC stabilization which is mentioned in previous section. The simulation of plasma with ASTRA code is performed using the available experimental data as the description of table 1. The electron and ion temperature profiles are obtained from the ECE and XCS diagnostic respectively and plasma rotation profiles are also obtained XCS. The profile information which is not available from the experiment is estimated or evaluated with the code. The density profile is assumed matching usual L-mode profile, the line averaged value and plasma total stored energy. The current density or q – profile evolution is evaluated with ASTRA code with the initially assumed q – profile. The initial q – profile

Table 3.1 Settings of plasma parameters for simulation of pulse 6272

Plasma current [MA]	0.429	n_e	Estimated to match the W_{tot}
Toroidal field [T]	2.0	T_e	From ECE (t = 5 s)
ECH/CD frequency [GHz]	110 (X-mode)	T_i	From XCS (t = 5 s)
ECH/CD power [MW]	0.280	P_{rad}	Bremsstrahlung, Cyclotron, Line (Carbon)
ECH/CD launcher location (R, Z) [M]	(2.80, -0.252)	V_{tor}	From XCS (t = 5 s)
ECH/CD launcher angle	$\theta = 61.3°$ $\varphi = 200°$	V_{pol}	Neoclassical
Seed island width [cm]	8.0	Initial q	Estimated as parabolic profile
Z_{eff}	2.0	j_{bs}	Sauter's formula

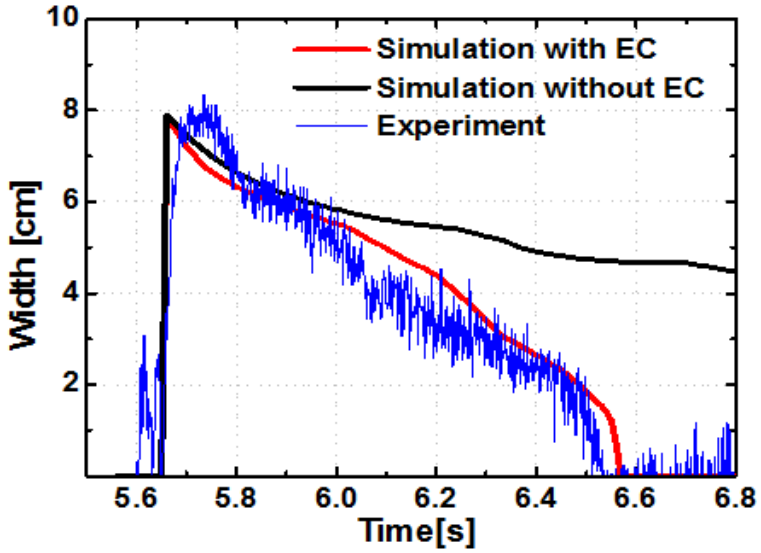

Figure 3.6 Evaluation of island width evolution from experiment(blue line) , simulation of pulse 6272 (red line) and simulation without EC case (black line).

is assumed as parabolic profile which is proper enough to matching the q =1 and q = 2 position of the experiment. For evaluation of bootstrap current density, the Sauter's formula is introduced. The EC absorption and current drive calculation is performed just for the 110 GHz EC because the power deposition of X3 mode is much lower than the X2 mode injection. MRE solver is started when the mode signal appears and the seed island width is assumed to match the experiment result. The simulation is started at t = 4 s in experimental time and the time step is assigned at most 0.001 s.

The simulation result of the island width evolution is in the figure 3.5. The island width in the experiment is calculated with the formula in section 3.1 using the mirnov coil signal data and other information of plasma variation is

obtained from the simulation result such as magnetic shear and position in minor radius of rational surface since the experimental measurement is not available. This experimental island width is compared with the island width in simulation which is evaluated from the MRE solver in the dimension of meter. The simulation result agrees well with the experiment result showing the stabilization effect of EC injection. Based on this, this integrated numerical system is expected to reproduce the island width behavior with EC so that it is used for predictive NTM stabilization simulations with feedback control.

Chapter 4

NTM stabilization simulation via growth rate seeking method

4.1 NTM stabilization simulation using minimum growth rate seeking control

4.1.1 Minimum growth rate seeking controller

To perform control simulation and confirm the effectiveness of the minimum growth rate seeking method, two type of controller are introduced in this work; finite difference method (FDM) based minimum seeking controller and sinusoidal perturbation based minimum seeking controller. The detail settings of controllers as follow.

The FDM based controller is established to move angle to the minimum growth rate direction with a step which is same as the magnitude of the gain. When the growth rate is obtain from the diagnostic, the gradient detector estimates the gradient between the growth rate and poloidal angle with FDM by memorizing the previous time step values. This estimated gradient is converted to the sign element from switching element. This determines the direction or sign of next step poloidal angle variation. Finally the time variation rate of poloidal angle is obtained by multiplying the adaptive gain

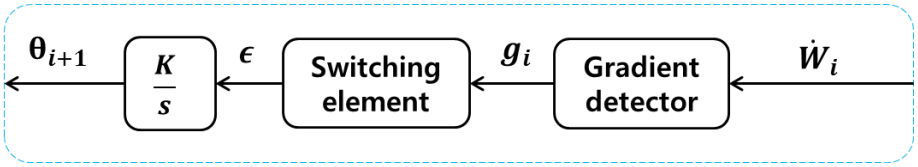

Figure 4.1 Control block diagram of finite difference method based minimum growth rate seeking controller.

and the sign element and poloidal angle of next step is deduced. The switching element is not included in usual minimum seeking problems so that the time variation of output is obtained as the multiplication of adaptive gain and gradient itself which is introduced in previous section as the steepest decent method. However, for minimizing the growth rate of mode, this moving law makes the controller to be quite unstable since the minimum of growth rate is time varying and the gradient is not zero at the minimum point. The controller can make output to move significantly although it is around the minimum point and this can cause the significant reduction of control performance. Therefore, the moving law is corrected to use the sign of gradient instead of the value itself and the moving step is determined by just the adaptive gain.

$$\theta_{i+1} = \theta_i + K\, sign(g_i) \tag{4.1}$$

Here, i is the time step index, K is the adaptive gain and g is gradient between the growth rate and poloidal angle. The value of adaptive gain needs to satisfy the minimum seeking condition which is mentioned in chapter 2. Therefore, the sign of adaptive gain is determined to negative and the magnitude of gain is selected by scanning of gain from the simulations to

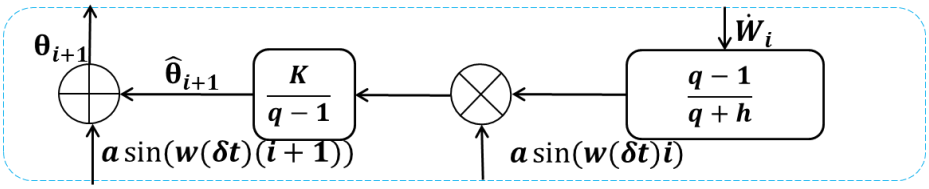

Figure 4.2 Control block diagram of sinusoidal perturbation based minimum growth rate seeking controller.

stabilize NTM as fast as possible. And this is interpolated linearly with island width as the gain adjusting method to reduce the steady state error gradually.

The sinusoidal perturbation based minimum seeking controller is established to move angle to the minimum growth rate direction on average of perturbation time. The sinusoidal perturbation based minimum seeking control requires the sinusoidal signal and frequency filtering but this can be performed with discrete numerical calculation as follow. The growth rate from the diagnostic is filtered out with 1st order high pass filter whose performance is determined by the cut-off frequency, h. This removes the offset of input signal. The sinusoidal value of that time step is multiplied after that. By integrating the resulting value, the signals with high frequency is removed and this filtered value is multiplied by adaptive gain. This makes the estimation value of proper poloidal angle and finally sinusoidal value for the next time step is added for probing process. The total calculation procedure is as follow.

$$\dot{W}_{i,h} = -h\dot{W}_{i-1,H} + \dot{W}_i - \dot{W}_{i-1} \tag{4.2}$$

$$\dot{W}_{i,M} = \dot{W}_{i,H}\, a\sin(w(\delta t)i) \tag{4.3}$$

$$\hat{\theta}_{i+1} = \hat{\theta}_i + K\,\dot{W}_{i,M} \tag{4.4}$$

$$\theta_{i+1} = \hat{\theta}_{i+1} + a\sin(w(\delta t)(i+1)) \tag{4.5}$$

Here the subscription *i* is the time step index, H means the high pass filtered and M means multiplied by sinusoidal value. *h* is the cut-off frequency for high pass filter. *a* is the amplitude of sinusoidal perturbation and *w* is the frequency of perturbation. δt is the time interval of controller. $\hat{\theta}$ is the estimated proper poloidal angle and θ the output value which is added by sinusoidal perturbation. The *h*, *a*, *w* and *K* have to be selected properly considering the physical conditions of mode evolution. The magnitude of *a* is set as 0.1 to obtain small steady state error and sound adaptation of minimum point variation. The frequency *w* is set to make the perturbation period to be the order of 100 ms which is slow enough to catch the island width evolution so that the measurement of growth rate is possible and to realize the perturbation motion in simulation. The cut-off frequency, h is set as the 1 percent of perturbation frequency to avoid the attenuation of perturbation signal amplitude. Also the adaptive gain is set as negative value satisfying the condition mentioned in chapter 2 and the magnitude is selected as the fastest stabilization case from the various gain scanning simulation like FDM controller case.

4.1.2 Control simulation method

The imaginary KSTAR plasma is assumed to obtain 2/1 mode NTM which is proper to apply the controller. The toroidal magnetic field intensity is set as 2.65 T to use X2 mode 170 GHz EC which is planned to be used as the main actuator for NTM stabilization in KSTAR. The plasma current is set as

Table 4.1 The specification of ECCD settings in the stabilization simulation which satisfies present limitation of 170 GHz EC in KSTAR

Frequency	170 GHz
Power	(effectively) 800kW
Injecting mode	X2 mode (B_T = 2.5 - 3.5 T)
Poloidal beam angle	50° to 90°
Toroidal beam angle	+20°
Steering mirror speed	10°/s

600 kA and injection of 5 MW NBI is assumed to obtain high beta plasma which makes NTM to be more destabilized. The 4 cm of initial seed island is assumed to induce the NTM and the controller turns on after 100 ms for mode detection rough beam alignment. This initial beam alignment is assumed that the good initial poloidal angle of EC beam which is enough to affect to the island can be known roughly. The control algorithm to find this good enough initial poloidal angle is necessary in experiment. However, this is not the out of scope of this thesis and it is assumed that it already exists. The two cases of initial angle conditions are tested. One is the case of initial poloidal angle of 62 degree. This is misaligned about 3 cm from the left hand side of island O-point. The adaptive gain is scanned and optimized with this case of initial poloidal angle. The other is case of 61 degree which is misaligned about 2 cm from the right hand side of island O-point. The EC driven current density profile changes significantly with angle variation in this case of initial poloidal angle. This case is to confirm the effectiveness of

controller for different condition. Other details of EC injection is described in table 2. The control loop time is set as 20 ms and island growth rate is measured every 1 ms in simulations

4.1.3 Results of NTM stabilization simulation using minimum growth rate seeking control

. The simulations with EC injection and without feedback control are performed. The resulting island width evolution is shown in figure 4.3. For the 62 degree of initial poloidal angle case, the stabilizing effect of EC is not

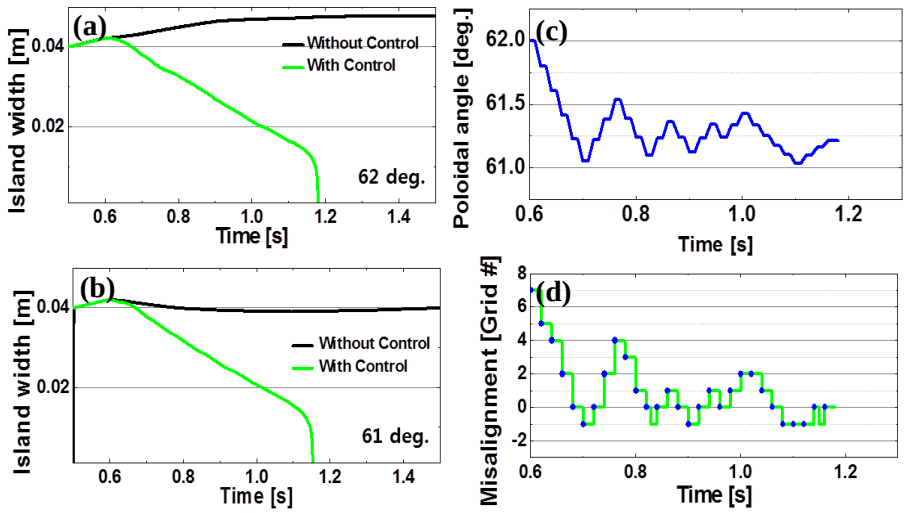

Figure 4.3 The simulated island width behavior using FDM based minimum growth rate seeking controller for (a): initial poloidal angle of 62 degree and (b): initial poloidal angle of 61 degree. (c): Time evolution of controlled poloidal angle for (a) simulation and (d): time evolution of resulting misalignment.

observed although the EC is injected inside the island. This is because the misalignment reduces efficiency of stabilizing EC and destabilizing effect of bootstrap current perturbation is larger than stabilizing effect as a result. For the 61 degree of initial poloidal angle case, the EC stabilize the mode slightly. However the effect is very insufficient to achieve the full stabilization of mode.

On contrast, the full stabilization of mode is successfully achieved applying the minimum growth rate seeking and FDM based feedback controller for both cases of initial poloidal angle. The resulting island width

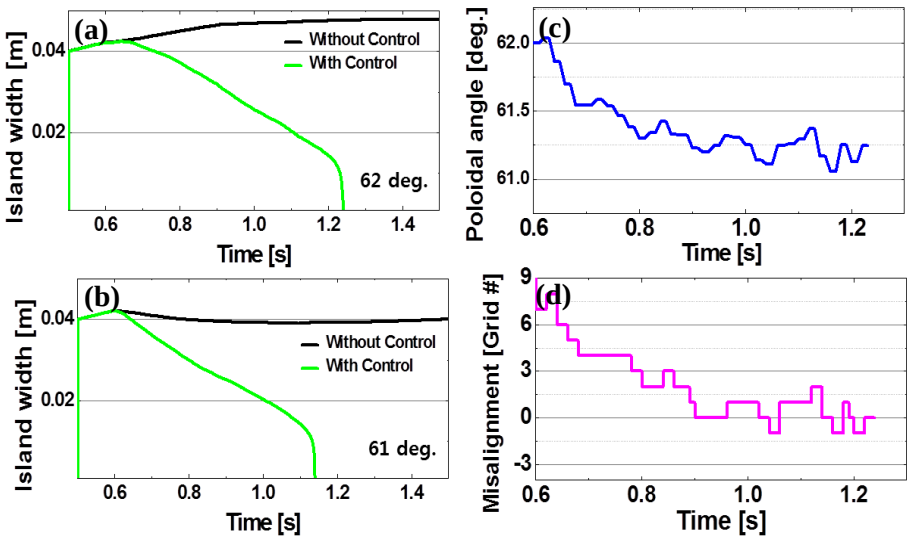

Figure 4.4 The simulated island width behavior using sinusoidal perturbation based minimum growth rate seeking controller for (a): initial poloidal angle of 62 degree and (b): initial poloidal angle of 61 degree. (c): Time evolution of controlled poloidal angle for (a) simulation and (d): time evolution of resulting misalignment.

evolution is shown in figure 4.3. Although the target angle is not assigned, the misaligned initial angle is adjusted to the more proper angle decreasing monitored growth rate. This makes it possible to stabilize mode totally. The angle moves to the growth rate decreasing direction. The misalignment converges to zero at first because the growth rate is reduced as the misalignment decreases. After the poloidal angle arrives zero misalignment point, the controller doesn't stop and moves one more step to the same direction. This is not the favorable control but necessary to estimate the minimum point. When the growth rate is increased at this step, the controller changes its direction to reduce the growth rate and misalignment. Therefore, the controller oscillates around zero misalignment point with error after arriving that point firstly. However, sometimes the controller misaligns the poloidal angle more than expected. This is due to the effects of indirect measurement and variation of EC driven current profile. The island growth rate is estimated from the virtual measurement of mirnov coil signal. Since it is affected by the q – profile and mode position, the change of estimated growth rate can be different with that of real growth rate. Also the real growth rate can be reduced although the misalignment is increased. Variation of plasma equilibrium can change the EC driven current profile to increase. This reduces the value of whole map between the poloidal and growth rate so that the controller lose its right direction for a while. But these distorting phenomena are recovered soon by the minimum seeking algorithm and controller regulates around zero misalignment point in the end which is intended.

The sinusoidal perturbation based controller with minimum growth rate seeking also successes to stabilize the mode totally for both cases of initial

poloidal angle. The poloidal angle is adjusted with the small amplitude of sinusoidal perturbation. The controller works well and averaged angle approaches to the angle where the misalignment is zero gradually as a result. The sinusoidal perturbation based minimum seeking also requires the perturbation to estimate the minimum point. This makes the steady state error but the controller regulates around zero misalignment point stably. Although there is same risk of false measurement or slight change of plasma condition, the sinusoidal perturbation based controller filters out the effects of poloidal angle or misalignment variation well and the significant miss of control is not observed.

For both type of minimum seeking controller, the stabilization of NTM is achieved. The roughly known initial poloidal angle is adjusted by this feedback controller to the more proper angle value which is unknown. By minimizing the growth rate, the misalignment is reduced and converged around zero which is most favorable for the fastest NTM stabilization. Based on these results, it can be known that the control using minimum growth rate seeking method is effective and successful for full stabilization of NTM.

4.2 Comparison with minimum width seeking control

The minimum growth rate seeking method is expected to be more efficient than the minimum width seeking method for aligning poloidal angle and stabilizing the NTM since the growth rate has more clear minimum relation with poloidal angle than island width. To confirm this expectation, the stabilization simulations using minimum width seeking controller are

performed to be compared with that of minimum growth rate seeking controller. Two type of minimum seeking controller is used same as simulation using minimum growth rate seeking method. For the FDM based controller, the same controller is introduced. For the sinusoidal perturbation based controller, the adaptive gain is changed to obtain the optimized stabilization result. The initial poloidal angle is assumed as 62 degree.

4.2.1 Results of FDM based minimum seeking controller

The minimum width seeking method realized with the FDM based controller is failed to stabilize the mode. The island width is decreases as the controller is turned on. The saturation of island width is observed in the middle of the stabilization but the width is gradually reduced as it is intended for about 800 ms. The island width suddenly increases significantly after that. And the misalignment is decreased at first after controller onset. However, the controller just passes the zero misalignment point and the misalignment increases as a results. The misalignment is reduced again after the island width is increased. This repeats causing huge oscillation of misalignment around zero misalignment point. And the controller loses its control suddenly when the misalignment is increased significantly.

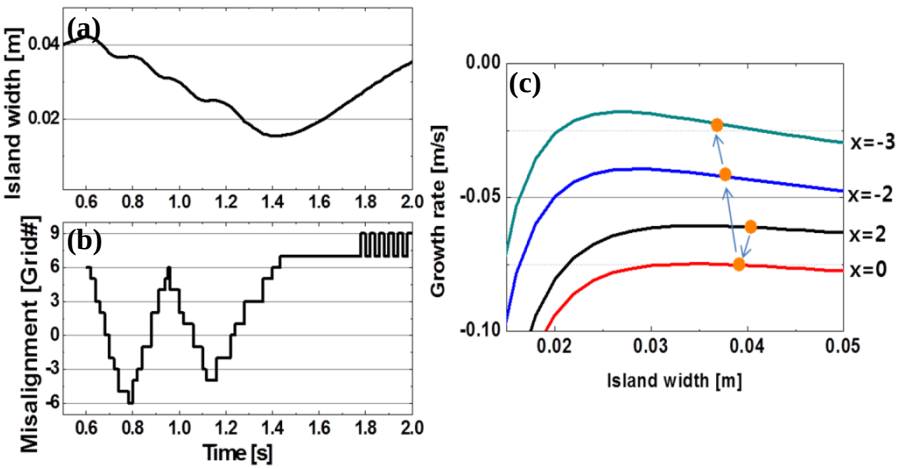

Figure 4.5 The simulated island width behavior using FDM based minimum width seeking controller for (a): initial poloidal angle of 62 degree and (b): time evolution of resulting misalignment. (c): Time evolution of mode stability (x: misalignment in dimension of grid, orange point: state of mode in order t = 0.68, 0.70, 0.72, 0.74 s).

The degradation of this minimum width seeking controller is usually caused from the huge oscillation of misalignment. This is due to the absence of obvious minimum width with respect to the poloidal angle. When the controller is turned on and poloidal angle is adjusted from its initial value the island width is decreased although the angle is not sufficiently aligned to be around zero misalignment point. This makes the controller to estimate the gradient incorrectly. Figure 4.5 shows more details for the dynamics this controller for t = 0.68 s to 0.74 s when the first passing the zero misalignment point is happened. The poloidal angle is misaligned at t = 0.68s and the controller moves the poloidal angle to the misalignment decreasing direction to minimize the island width at t = 0.70 s. Because the island width also is

decreased, the controller consider that the previous direction is right to achieve minimization and the misalignment is increased one more step as it is intended. For the correct control, the input value has to increase at this step. However the island width keeps decreasing because of its negative growth rate in spite of the misalignment. The controller doesn't the moving direction of poloidal angle because of this although the direction is the misalignment increasing direction. As a result, the misalignment increases and when it becomes large to reduce the stabilizing effect of EC significantly, the island width starts to grow. After that, the controller can switch the moving direction. Furthermore, the distortion of width measurement can happen in this simulation and this make the switching of direction makes slow due to the variation of island width could be small to overcome this distortion when the EC is significantly misaligned to affect the island width evolution. Also there is the risk of local minimum. As it is mentioned above, island width can grow when the misalignment is large enough. The controller changes direction at that moment. However if the misalignment keep growing due to the unexpected plasma variation or false measurement from mirnov coil diagnostic, the controller cannot recover the proper angle condition. This is because that the growth rate is positive above the some level of misalignment. This is opposite case with figure 4.4. When the misalignment is larger than some level, the island width always grows whether the misalignment is increased or decreased. This makes the controller change its direction every control time step and the output value cannot converge to the real minimizing solution. To avoid this, at least, staying the angle to make the growth rate negative is favorable. The FDM based minimum width seeking controller cannot accept this recommendation since this controller needs the point of

positive growth rate which makes the island width to be saturated and increased.

The FDM based minimum width seeking controller requires the saturation of island width to obtain the proper control. The controller is improved by adding the saturation checking step to reduce the oscillation of poloidal angle or the misalignment. The stabilization of mode is successfully achieved by this improved controller as a result. The island width is gradually reduced and fully suppressed. The time for this full stabilization is longer than that of simulation using FDM based minimum growth rate seeking control. The resulting misalignment shows the perturbations although the poloidal angle is not changed. This is caused by the time-dependent plasma variation and the controller successfully reduced misalignment level directing the zero

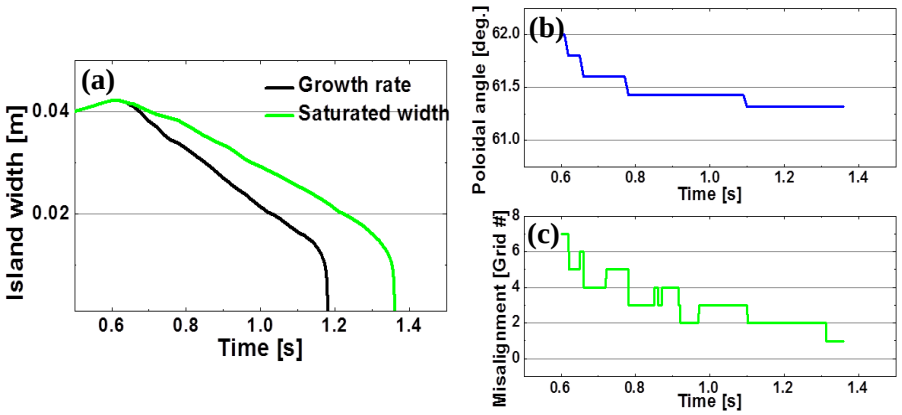

Figure 4.6 The simulated island width behavior using FDM based minimum saturated width seeking controller for (a): initial poloidal angle of 62 degree. (b): Time evolution of controlled poloidal angle and (d): time evolution of resulting misalignment.

point. However the speed of convergence is quite slow. The moving direction of controller is proper. But the controller has to wait for the saturation of the island width for the next control step to change the poloidal angle. The time for reducing misalignment to zero is increased. And the reducing velocity of island width cannot be faster than the minimum growth rate seeking controller since the growth rate of mode increases from the negative value to zero while the controller is waiting for the saturation of island width. Consequently, the minimum width seeking method using FDM based controller is not efficient than the minimum growth rate seeking method using same controller whether the island width saturation checking is added or not. This is because that the minimum island width with respect to the poloidal angle is only achieved as the form of saturated island width and the time for saturation degrades stabilizing efficiency.

4.2.2 Results of sinusoidal perturbation based minimum seeking controller

The minimum width seeking method realized with the sinusoidal perturbation based controller succeeds to stabilize the mode. The island width is decreased as the controller is turned on and fully stabilized. However this takes longer than the stabilization through the same sinusoidal perturbation based minimum growth rate seeking controller. This can be discovered by the adaptive gain scan. Since the scale of growth rate is larger than that of island width as order of 0.1 and order of 0.01 respectively, the adaptive gain should be changed when the input parameter is changed from the growth rate to the

island width. When the adaptive gain increases, the speed of convergence also generally increases. But the limitation of actuator such as the maximum velocity of angle moving should be considered. Therefore, large enough adaptive gain considering the limitation is required and this is selected by gain scanning to compare the two methods for NTM stabilization; minimum growth rate seeking and minimum width seeking. The achievable shortest time for stabilization is longer for the minimum width seeking method like figure 4.7.

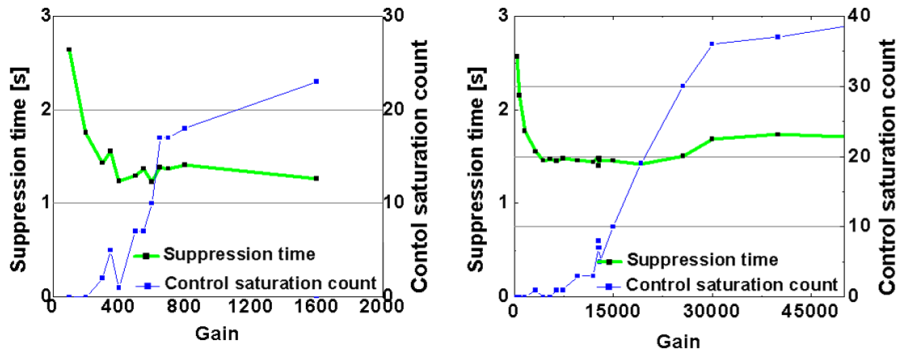

Figure 4.7 Full suppression time for adaptive gain scan (green) and counts when the controller is limited by the maximum speed of angle moving (blue) for (a): sinusoidal perturbation based minimum growth rate seeking controller and (b): sinusoidal perturbation based minimum width seeking controller.

The figure 4.8 shows the fastest case of minimum width seeking method using sinusoidal perturbation based controller. The poloidal angle is controlled with added sinusoidal perturbation making the misalignment also have the sinusoidal perturbation motion. The misalignment is decreased as a result. This is notable considering the failure of full stabilization of mode using FDM based minimum width seeking controller. The reason of this successful stabilization is conjectured as the sinusoidal perturbation based controller can extract the responsive signal. The sinusoidal perturbation of the poloidal angle makes the perturbation of misalignment and this cause the perturbation of the growth rate based on the modeling study of NTM. The resulting perturbation of the growth rate can be sine wave or not. If it can be assumed as sinusoidal perturbation, the width can show the cosine wave as a result. This is guessed

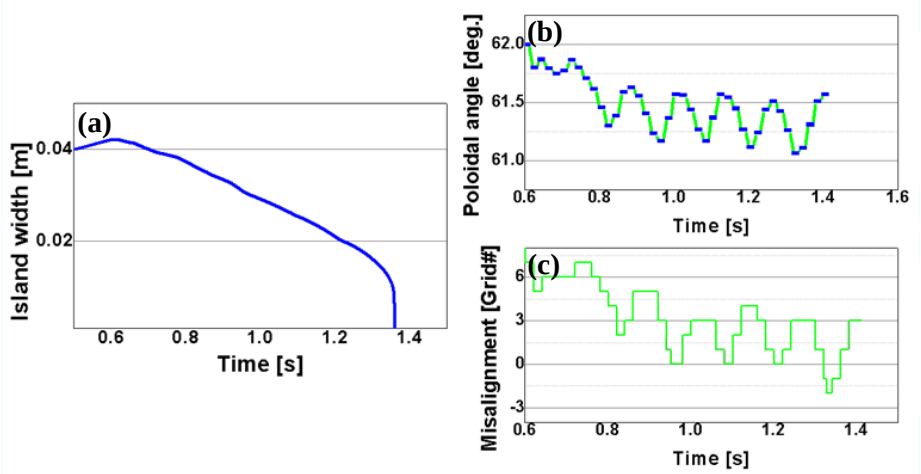

Figure 4.8 The simulated island width behavior using sinusoidal perturbation based minimum width seeking controller for (a): initial poloidal angle of 62 degree. (b): Time evolution of controlled poloidal angle and (d): time evolution of resulting misalignment.

to make it possible to fine the right direction for controller to reduce the misalignment by filtering out this resulting signal.

The misalignment decreases fast for the first about 200 ms. The reducing speed is slow down after that preventing the misalignment approach to the zero. The finally obtained misalignment value is 1 for number of radial grid on average of sinusoidal perturbation. This is inferior as compared with misalignment result for simulation using same sinusoidal based minimum growth rate seeking controller in figure 4.4. This is also observed for the larger adaptive gain than case in figure 4.9. Therefore, it is expected that the change of input parameter from the growth rate to island width makes this difference. The reason of the retardation of misalignment convergence is conjectured as follow. Because the resulting width variation is the integration of the growth rate in time, this can contain the phase shift. Also the order of signal which is function of time can be raised and this makes shape of signal to be more complex than that of growth rate signal to filter out the proper value for tested controller in this thesis. However, the furthermore study is necessary for exact cause of that.

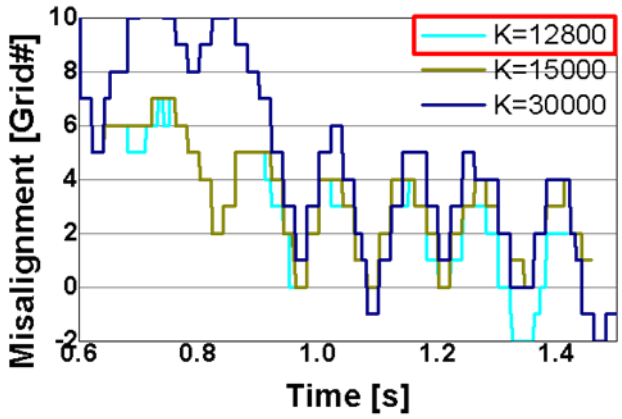

Figure 4.9 Time evolution of misalignment for the sinusoidal perturbation based minimum width seeking controller with the adaptive gain K=12800 (fastest case), 15000 and 30000.

Based on these results, using the growth rate as the input for minimum seeking method is efficient than using the width for both types of minimum seeking controller. The minimum growth rate seeking method also less limited for the type of seeking controller. Unlike the minimum growth rate seeking method, the minimum width seeking method is failed to stabilize the mode for FDM based controller.

Chapter 5

Conclusion

The minimum island growth rate seeking control concept is proposed and its performance is evaluated by comparing with the conventional island width control for feedback stabilization of NTMs. As a first step, control using the minimum island width seeking method has been studied to avoid the massive measurement or calculation and reduce the misalignment between the EC beam deposition position and island position for NTM stabilization. Assuming that the island width has minimum with respect to the misalignment or the EC launcher poloidal angle which can change the misalignment actively by changing the EC deposition position, this method minimizes the island by tuning the misalignment. However if the control loop time is small so that the controller does not wait until the island width is saturated, the minimum relation between the misalignment and the island width is unclear making the assumption break down. On the other hand, the island growth rate has stronger relation with the misalignment than the island width, the growth rate decreases as the misalignment is reduced, which is identified by numerical modelling studies. Therefore, the control strategy using minimum growth rate seeking method is newly proposed and studied its effectiveness by time-dependent numerical simulations in this thesis. Firstly, an integrated numerical system is setup where plasma equilibrium, transport, and heating and CD by EC are coupled with the solver of simplified Rutherford equation

in a self-consistent way. The NTM stabilization experiment in KSTAR is analyzed and is tried to be reproduced by this numerical system. The integrated numerical system successfully reproduced the island width behavior of. Using this, the stabilization simulation using proposed feedback control method is performed with two types of the minimum seeking controller. One is the FDM based minimum seeking controller and the other is sinusoidal perturbation based controller. The input is set as the growth rate assumed to be measured from the mirnov coil by considering variation of the plasma conditions and the output is set as the poloidal angle of the EC beam injection to reflect the real control situation in experiments. The full stabilization of mode is achieved by applying both types of controller with the minimum growth rate seeking method. The controller adjusts the poloidal angle reducing the misalignment around zero successfully. To investigate the effectiveness of minimum growth rate seeking than minimum width seeking, the simulations using minimum width seeking method is also performed for comparison. FDM based minimum width seeking controller failed to stabilize the mode sometimes as expected. Since the unsaturated island width doesn’t have clear minimum relation with the poloidal angle, the controller couldn’t find the correct direction to reduce the misalignment. This controller is improved by adding an island width saturation checking step. As a result, the poloidal angle is controlled well and full stabilization is achieved. However, the stabilization time is extended to about 200 ms than the minimum growth rate seeking method due to extra time consumed for waiting island width saturation. The sinusoidal perturbation based minimum width seeking

controller is successful in full stabilization but slower and less accurate than the minimum growth rate seeking method. This is conjectured that because the perturbation and filtering which are introduced in the controller can extract the response of the growth rate indirectly so that the efficiency is degraded than using the growth rate directly though the stabilization is obtained. This requires furthermore investigation. Therefore, the newly proposed minimum growth rate seeking method is thought be more effective strategy for NTM stabilization compared with the minimum width seeking method in terms of stabilization speed and robustness.

Based on these results, control with the growth rate as the input and the poloidal angle as the output using minimum seeking can be applied as a new control scheme to KSTAR and ITER which does not require detailed information of the island or EC beam but a rough position of the mode. Furthermore studies such as for the case of noisy measurement of input and the optimization of controller by changing perturbation signal form, the frequency of that or filtering method are necessary in the future.

Bibliography

[1] R.J. La Haye, "Neoclassical tearing modes and their control", Phys. Plasma 13, 055501 (2006)

[2] R. J. Buttery, et al., "Neoclassical tearing modes", Plasma Phys. Control. Fusion 42 B61 (2000)

[3] R.J. La Haye, et al., "Control of neoclassical tearing modes in DIII-D", Phys. Plasmas 9, 2051 (2002)

[4] R. Prater, et al., "Discharge improvement through control of neoclassical tearing modes by localized ECCD in DIII-D", Nucl. Fusion 43 1128 (2003)

[5] A. Isayama, et al., "Complete stabilization of a tearing mode in steady state high-β_p H-mode discharges by the first harmonic electron cyclotron heating/current drive on JT-60U", Plasma Phys. Controlled Fusion 42 L37 (2000)

[6] A. Isayama, et al., "Achievement of high fusion triple product, steady-state sustainment and real-time NTM stabilization in high-β_p ELMy H-mode discharges in JT-60U", Nucl. Fusion 43 1272 (2003)

[7] R. J. La Haye et al., "Requirements of alignment of electron cyclotron current drive for neoclassical tearing mode stabilization in ITER", Nucl. Fusion 48 054004 (2008)

[8] M. Reich et al., "ECCD based NTM control at ASDEX Upgrade", 39th EPS (2012)

[9] Humphreys D. A. et al., "Active control for stabilization of neoclassical tearing modes", Phys. Plasma 13, 056113 (2006)

[10] W. Wehner, E. Schuster, “Stabilization of neoclassical tearing modes in tokamak fusion plasmas via extremum seeking”, 18th IEEE International Conference on Control Applications (2009)

[11] W. Wehner, E. Schuster, “Control-oriented modelling for neoclassical tearing mode stabilization via minimum-seeking techniques”, Nucl. Fusion 52 074003 (2012)

[12] Her-Terng Yau, Chen-Han Wu, “Comparison of extremum-seeking control techniques for maximum power point tracking in photovoltaic systems”, Energies 4(12), 2180-2195 (2011)

[13] Chunlei Zhang, Raul Ordonez, “Extremum-Seeking Control and Applications: A Numerical Optimization-Based Approach”, Springer (2011)

[14] K. Ariyur, M. Kristic, “Real-time optimization by extremum-seeking control”, Wiley (2003)

[15] Rutherford P. H. “Nonlinear growth of the tearing mode”, Phys. Fluids 16, 1903 (1973)

[16] E. Westerhof, “Tearing mode stabilization by local current density perturbations”, Nucl. Fusion 30 1143 (1990)

[17] R. J. La Haye, et al., “Cross-machine benchmarking for ITER for neoclassical tearing mode stabilization by electron cyclotron current drive”, Nucl. Fusion 46 451 (2006)

[18] R. J. La Haye, et al., “Dimensionless scaling of the critical beta for onset of a neoclassical tearing mode”, Phys. Plasma 7, 3349 (2000)

[19] Y.-S. Na, et al., “Real-time control of neoclassical tearing mode in time dependent simulation on KSTAR”, 23th IAEA Fusion Energy Conf. (2010)

[20] C. N. Nguyen, et al., “Simulation of saturated tearing modes in tokamaks”, Phys. Plasma 11, 3460 (2004)

[21] F. W. Perkins, et al., Proc. 24th EPS Conf. on controlled Fusion and Plasma Physics (1997)

[22] D. De Lazzari, et al., “On the merits of heating and current drive for tearing mode stabilization”, Nucl. Fusion 49 075002 (2009)

국문초록

신고전 찢어짐 모드(NTM)는 높은 성능의 플라즈마를 얻기 위해서 안정화해야 하는 불안정성 중에 하나이다. NTM은 플라즈마 가둠 성능을 떨어뜨리고 때로 플라즈마 붕괴를 일으키는 원인이 될 수 있다. NTM을 안정화하는데 국소적인 전자 사이클로트론 전류 구동(ECCD)을 입사해 모드의 원인이 되는 부트스트랩 전류의 손실을 보상하는 방법이 효과적인 것으로 실험적으로도 증명되어왔다. 이 방법의 효율은 NTM에 의해 발생한 자기섬과 EC 빔의 정렬에 크게 영향을 받는다. 따라서 NTM을 효율적으로 얻기 위해서는 실시간 되먹임 제어가 필수적이다.

이 논문에서는, 최소 증가율 탐색 기법을 이용하는 실시간 되먹임 NTM 제어 개념을 제안하였으며 이는 최소 자기섬 너비 탐색 기법을 이용하는 것 보다 더 빠르고 효과적이었다. 최소 증가율 탐색 기법은 비 모델기반 제어 방법으로 정확한 실시간 평형 재구축이나 EC 빔 계산, 또는 NTM 플라즈마에 대한 모델 식별(Identification)이 필요하지 않다.

제어 전산모사를 위해 시간의존적 NTM 변화 모사를 위한 통합 수치 모델이 확립되었다. 여기에는 플라즈마 평형, 수송 그리고 EC에 의한 가열 및 전류구동이 간소화된 Rutherford 식 계산에 결합되어있다. 이 통합 수치 모델을 KSTAR 플라즈마에 적용하여 실제 NTM 안정화 실험에서의 자기섬 변화를 모사하였다.

제안한 제어 개념의 성능을 평가하기 위해 두 가지 타입의 최소 탐색 제어기(Finite difference method 기반 제어기, Sinusoidal perturbation 기반 제어기)를 이용해 되먹임 제어 전산모사를 수행하였다. 실제적인 인풋과 아웃풋 인자로 각각 진단 장치에서

측정된 자기섬 증가율과 폴로이달 입사 각의 형태로 사용되었다. 이 결과들은 최소 자기섬 탐색 방법을 이용한 전산모사 결과와 비교되었다. 그 결과 더 짧은 시간 규모에서 새로 제안된 제어 방법이 최소 탐색 제어기의 종류에 덜 제한되며 더 강건하게 EC 빔을 정렬하는 것으로 드러났다.

주요어: 신고전 찢어짐 모드, 자기섬, NTM 안정화, 최소 탐색 제어, 전자 사이클로트론 전류 구동 (ECCD)

학 번: 2012-20988